Published in final edited form as:

Lab Chip. 2011 December 21; 11(24): 4274–4278. doi:10.1039/c1lc20758j.

Two-dimensional Paper‡ Networks: programmable fluidic disconnects for multi-step processes in shaped paper

Barry R. Lutz[a], **Philip Trinh**[a], **Cameron Ball**[a], **Elain Fu**[a], and **Paul Yager**[a]

Barry R. Lutz: blutz@uw.edu

[a]Box 355061, Department of Bioengineering, University of Washington, Seattle, WA. Fax: 1-206-616-3928; Tel: 1-206-685-9891

Abstract

Most laboratory assays take advantage of multi-step protocols to achieve high performance, but conventional paper-based tests (e.g., lateral flow tests) are generally limited to assays that can be carried out in a single fluidic step. We have developed two-dimensional paper networks (2DPNs) that use materials from lateral flow tests but reconfigure them to enable programming of multi-step reagent delivery sequences. The 2DPN uses multiple converging fluid inlets to control the arrival time of each fluid to a detection zone or reaction zone, and it requires a method to disconnect each fluid source in a corresponding timed sequence. Here, we present a method that allows programmed disconnection of fluid sources required for multi-step delivery. A 2DPN with legs of different lengths is inserted into a shared buffer well, and the dropping fluid surface disconnects each leg at in a programmable sequence. This approach could enable multi-step laboratory assays to be converted into simple point-of-care devices that have high performance yet remain easy to use.

1. Introduction

Devices fabricated from paper or other wicking material provide an inexpensive “microfluidic” platform for chemical analysis or medical diagnostics without the need for pumps or other equipment. The classic example is the lateral flow test (LFT), which uses a single strip of paper with dried reagents to provide visual detection of analytes in an easy-to-use format. Recently there has been resurgence in development of wicking-based devices that expand the functionality beyond that of conventional LFTs[1–21]. One prominent class of devices uses branched wicking channels to split a sample into discrete zones containing different test chemistries[9–21]. The advantage over conventional LFTs is that multiple tests (and controls[10, 17]) can be performed on a single device. However, all of these methods have thus far been limited to assays that can be carried out within a single chemical delivery step, just as with conventional LFTs. In contrast, nearly all laboratory assays involve a timed

‡We use the term “paper” broadly to describe porous materials used as wicking materials and assay substrates in diagnostics. Nitrocellulose used here is not technically classified as paper.

Correspondence to: Barry R. Lutz, blutz@uw.edu.

†Electronic Supplementary Information (ESI) available: Figure S1 – fluid wicking into cellulose and nitrocellulose strips. Figure S2 – fluid shut off without a regulating wick. Figure S3 – gravity effects in wicking. See DOI: 10.1039/b000000x/

sequence of chemical steps to achieve high performance. For example, the classic enzyme-linked immunosorbent assay (ELISA) normally involves a timed sequence of manual pipetting steps including sample incubation, at least one analyte labeling step, and colorimetric development, with washes in between every step. This multi-step format has the advantages of improved sensitivity and specificity due to signal amplification and washes. However, multi-step assays like this have historically not been possible in a lateral flow format, and none of the emerging platforms above have been designed to carry out automated multi-step processes.

We have worked to introduce timing mechanisms into paper devices to "program" automated multi-step assays. Multi-step processes can be created by combining two basic functions: 1) controlling the *arrival time* of distinct reagents to a reaction zone or detection zone, and 2) controlling the *"shut off"* time of each reagent. In conventional microfluidic systems, multi-step processes are controlled by pumps and/or valves that start and stop each fluid in a timed sequence. We have shown that a shaped piece of paper, a two-dimensional paper network (2DPN), provides a platform for autonomous multi-step fluidic processing[22–26]. The convergence of multiple inlet legs allows different fluids to be delivered to a detection zone in a timed sequence, and it requires a method to disconnect each fluid source in a corresponding sequence. We previously reported disconnects that required individual fluid source pads on each leg of the 2DPN. Here, we present a method that allows programming of the disconnect sequence using a single shared well as the fluid source. Different reagents can be delivered by applying the desired dry reagent chemistry to each leg. The approach uses many of the same materials as classic LFTs, but timing events needed for automated multi-step processes are programmed into the device by the source well design and the shape of the 2DPN.

2. Experimental

A plastic housing was used to reduce evaporation (see below). The housing and fluid well were fabricated from a PMMA sheet (2.5 mm thick) and 0.25 mm thick Mylar film with adhesive coating on both sides (10 mil, Fraylock Inc, San Carlos, CA); materials were cut to shape by a CO_2 laser cutter (Universal Laser Systems, Scottsdale, AZ), assembled by hand, and pressed to seal the adhesive. Nitrocellulose membranes (Mylar-backed HiFlow Plus 135, HF13504, Millipore, Billerica, MA) and high fluid capacity cellulose pads (C083, Millipore) were cut using the laser cutter. All experiments used phosphate buffered saline with 0.05% Tween 20 (PBST) to which food coloring was added. Individual legs or a complete 2DPN were mounted on an adhesive plastic backing and then enclosed in the housing to create a cartridge. Flow was initiated by inserting the cartridge against a mechanical stop in the well. Fluid fronts were tracked manually from webcam videos recorded at one frame per second (Logitech, Fremont CA) using ImageJ[27].

3. Results and Discussion

3.1 Fluidic disconnects in isolated strips

Figure 1 demonstrates timed shut-off of fluid delivery in separate nitrocellulose strips ("legs"). Legs were arranged on an adhesive plastic backing within an enclosed cartridge

such that their ends protruded different amounts. A disposable dropper was used to fill the well to capacity; reproducibility of the fill step was measured by weighing well, 1.51±0.06 mL (±4%, n=10). The cartridge was designed such that it could be fully inserted against a mechanical stop; thus careful positioning by the user was not required. When the cartridge was inserted into the well, each leg was immersed to a different depth (leg immersion depth, *ID*, is indicated for leg 3). As the fluid level in the well dropped due to wicking, each leg was disconnected from the source fluid in a programmed sequence.

The disconnect timing is controlled via the fluid depletion rate, the leg immersion depth, and the cross-sectional area of the fluid well (when viewed from the top). In Figure 1, a separate high-capacity wick is added to regulate the rate of fluid depletion from the well ("regulating wick"). The timing and volume uptake can be further varied by using legs of different size, shape, fluid capacity, and/or wicking rate; here, we used a single material and legs of uniform width for simplicity.

Figure 1B shows the position of the liquid front in each leg as a function of time. The data are plotted in the form of the classic Lucas-Washburn equation describing 1D capillary uptake[28, 29]: $L^2 = Wt$, where L is the distance fluid has travelled into the material, t is time, and W is a coefficient that represents wicking properties of the fluid and material ($W = D\sigma\cos\theta/4\mu$; surface tension σ, contact angle θ, pore diameter D, fluid viscosity μ). Deviation from Lucas-Washburn wicking can occur due to gravity or evaporation. For perspective, the vertical wicking height $h_{max} = 4\sigma\cos\theta/\rho gD$ [30–32] for water in an 8 micron glass capillary (similar to nitrocellulose pore size) can be as high as 3 meters (*e.g.*, σ=0.0728 N/m, θ=20°, ρ=1 g/cm^3, g=9.8 m/s^2). In our experiments, gravity effects would be observed as a curvature in L^2 versus t plots (*i.e.*, wicking slows asymptotically on approach to $L=h_{max}$); the linearity of data in Fig. 1B suggests that gravity does not significantly affect wicking in these devices. To test for gravity effects more directly, we measured wicking of buffer in long nitrocellulose strips (20 cm) oriented vertically or horizontally – the L^2 versus t plots showed no observable curvature and were identical for the horizontal and vertical cases (see Supplementary Information). Thus, gravity does not have a significant effect on wicking for nitrocellulose devices of the scale used here (a few cm). Evaporation effects were controlled by enclosing devices in a plastic housing. Saturating the enclosed air in the device of Fig. 1 (5 cm x 12 cm x 0.15 cm) would require evaporation of <1 μL of water (~23 g H_2O/m^3 at 25ºC, ~50 g H_2O/m^3 at 40ºC for the worst case of initially dry air[33]). The humidifying wick provided a portion of this fluid. Delivered volumes for the legs in Figure 1 were approximately 15 μL (2.4 cm), 23 μL (3.8 cm), and 30 μL (4.9 cm). Thus, evaporation represented a small fraction of the delivered volumes in the enclosed devices.

As expected, Figure 1B shows that all legs followed the Lucas-Washburn line (black dashes, W=9.4 mm^2/s) until they were disconnected from the dropping fluid surface in the well (light diamonds and arrows). The fluid front advanced somewhat after the disconnection due to a period of equilibration of the fluid into the dry paper. The error in shut-off times for fluid delivery with these blunt-ended strips was 14–21 seconds (n=3, 5–20%). This error is comparable to the flow rate variability in the nitrocellulose membrane used here (+/−10%). Fluid delivery to each leg was shut off in a well-controlled and timed sequence.

In Figure 1, the rate that the fluid level in the well drops was dominated by the cellulose regulating wick that has a high fluid capacity and fast wicking rate. Specifically, the regulating wick drew fluid at ~7x the rate of the three nitrocellulose strips combined (see Supplementary Information). Before adopting the regulating wick, we performed experiments with nitrocellulose membranes only. To acheive shut of times similiar to those of Figure 1, the design without a regulating wick required minimizing the well cross-sectional area (thin and narrow when viewed from the top) and fabricating legs with very small differences in immersion depth. This design led to capillary bridges between the paper and the well surface as well as between adjacent paper strips, and the very small differences in immersion depths resulted in unreliable disconnection between leg tips and the fluid. We found that the reproducibility of shut off timing was improved by adding surfactant (we normally use surfactant in our assay buffers) and by using pointed leg tips. However, the timing errors were still large compared to those in Figure 1 when a regulating wick was used (see Supplementary Information).

The regulating wick is optional, but it provides several significant benefits. First, it allows the differential between leg immersion depths to be larger, which reduces the impact of device fabrication error. Second, when legs are interconnected in 2DPN designs (shown below), the regulating wick essentially decouples the design for shut-off timing from the details of device design. Thus, reagent volumes and assay connectivity are controlled largely via the 2DPN shape, while timing is controlled largely via the regulating wick and well design. Finally, the regulating wick helps to humidify the enclosed device to reduce evaporation and its associated timing errors.

3.2 Fluidic disconnects in a 2D paper network

The method in Figure 1 allows the fluid delivery in separate legs to be *shut off* at programmed times; the 2DPN design shown in Figure 2 connects these legs together to control the *arrival time* of each fluid to a common point, which could serve as a detection zone for an assay. When combined, these two functions provide autonomous multi-step fluid delivery. The complete device consists of a plastic housing containing the ready-to-use 2DPN and a shared buffer well. A single large cellulose absorbent pad was cut to serve multiple functions as 1) the regulating wick, 2) the absorbent pad at the end of the 2DPN, and 3) the humidifier. Three food colors dried on cellulose pads represent dried reagents to be rehydrated by the single buffer source. Operation of the device involves two simple steps: 1) filling the well to capacity with buffer from a disposable dropper, and 2) inserting the 2DPN cartridge into the well. It is important to note that device operation did not require special skill. First, the buffer volume was self-limiting; excess fluid overflowed from the well, and bubbles quickly escaped from the top. Repeated fill steps using the dropper gave 2.69 mL ± 0.05 mL (±2%, n=10). Second, the cartridge was designed to be fully inserted against a mechanical stop in the well so that no special positioning was required by the user. A single activation step initiated a pre-programmed sequence of timed fluid delivery steps without the need for further user intervention.

Figure 3 shows the automated delivery of three fluids to a detection zone (green box) after activation. In the first panel, the dried dyes are rehydrated and staged for sequential delivery,

and yellow fluid is delivered to the detection region. As in Figure 1, the lowering of the level of the fluid in the reservoir is dominated by the regulating wick; the location of the fluid front in the regulating wick is indicated in each panel. The second panel shows that the first leg (yellow) is disconnected from the fluid source, and the blue fluid is delivered to the detection zone. In the third panel, the first and second legs (yellow and blue) are disconnected from the fluid source, and the red fluid is delivered to the detection zone. Figure 3 (lower) plots the fluid color across the full strip width and within the detection zone as a function of time. Some “bleeding” can be seen at the lower edge of the strip (~20% of the paper width; Fig. 3 lower left); this is due to a small continued release of fluid from the cellulose reagent pads after shut off. Detection can be limited to the upper portion, where fluid delivery is distinct and uniform (~80% of the paper width; Fig. 3 lower right). We have found that different reagent pad materials (*e.g.*, glass fiber pads used in some LFTs) provide more distinct release profiles in pad-based delivery devices, so using these materials as reagent pads could reduce transients after shut off. Figure 3 shows that multiple fluids were delivered to the detection zone in a timed sequence with a total time that is appropriate for many common assays (30 minutes total). Compared to LFTs that are capable of only a single delivery step, the 2DPN can provide multi-step delivery of reagents needed for more sophisticated assays.

Variations in fluid viscosity or surface tension have linear impacts on the flowrate. For the case of dry reagents rehydrated by buffer, the resulting solution properties are predictable and reproducible, and these properties can be incorporated into the 2DPN design. As with LFTs, variation in sample properties can have a less predictable impact; expected variations can be incorporated into the 2DPN design by providing a sufficient time delay for sample delivery to be completed.

We showed previously that three legs can be used to deliver signal amplification reagents to a detection zone for an amplified immunoassay[22] using a different shut-off mechanism, *i.e.* individual volume-limited fluid source pads[22–24]. In that mechanism, source pads are pre-loaded with with fluid, similar to the well loading step described here. The fluid well method requires the device to stand (roughly) upright, while the pad method can be operated in any orientation. Both methods allow programming of shut of times in 2DPNs, and legs can be added to accomodate processes with more chemical steps.

Here, we used uniform-width legs and leg spacings and a simple regulating wick. The timing and volume uptake can manipulated by using legs of different size, shape, fluid capacity, and/or wicking rate. For example, decreasing the width of one leg would maintain the same approximate timing, but the volume delivered through that leg would be reduced due to increased fluidic resistance[23–25]. Further, wax-based time delays developed by the Phillips group[18] could be used to increase time delays in short legs. Timing steps for a given 2DPN design can also be manipulated by shaping the regulating wick to vary the time course of fluid depletion from the well. The shut-off method is compatible with paper devices fabricated by different 2D patterning methods (*e.g.*, knife cutting[34], wax printing[35], photoresist patterning[14, 36], shaped punches).

Conclusions

Laboratory assays normally use multi-step reagent sequences to achieve high performance. The combination of a 2DPN with a volume-limited fluid source provides the two basic functions needed to program timed processes for autonomous multi-step diagnostics: 1) controlled arrival time of reagents to a detection zone, and 2) controlled shut-off time of each reagent. This approach could enable a wide variety of multi-step laboratory assays to be converted into simple point-of-care devices that have high performance and are easy to use. Further, the multi-step programming could be combined with branched paper devices to add multi-step function to devices for multi-analyte detection[9–21], and complementary methods for flow control[18] and time indicators[17] could be similarly integrated into 2DPNs. Future work will be aimed at programming 2DPNs to carry out a variety of multi-step analytical tests.

Supplementary Material

Refer to Web version on PubMed Central for supplementary material.

Acknowledgments

We gratefully acknowledge NIH/NIBIB for funding this work through Challenge Grant 1RC1EB010593. We acknowledge Paolo Spicar-Mihalic for use of his nitrocellulose cutting method.

Notes and references

1. Pelton R. Bioactive paper provides a low-cost platform for diagnostics. Trac-Trends Anal Chem. 2009; 28(8):925–942.
2. Zhao WA, et al. Paper-Based Bioassays Using Gold Nanoparticle Colorimetric Probes. Anal Chem. 2008; 80(22):8431–8437. [PubMed: 18847216]
3. Dungchai W, et al. Electrochemical Detection for Paper-Based Microfluidics. Anal Chem. 2009; 81(14):5821–5826. [PubMed: 19485415]
4. Carvalhal RF, et al. Electrochemical Detection in a Paper-Based Separation Device. Anal Chem. 2010; 82(3):1162–1165. [PubMed: 20055490]
5. Nie ZH, et al. Electrochemical sensing in paper-based microfluidic devices. Lab Chip. 2010; 10(4): 477–483. [PubMed: 20126688]
6. Nie ZH, et al. Integration of paper-based microfluidic devices with commercial electrochemical readers. Lab Chip. 2010; 10(22):3163–3169. [PubMed: 20927458]
7. Apilux A, et al. Lab-on-Paper with Dual Electrochemical/Colorimetric Detection for Simultaneous Determination of Gold and Iron. Anal Chem. 2010; 82(5):1727–1732. [PubMed: 20121066]
8. Delaney JL, et al. Electrogenerated Chemiluminescence Detection in Paper-Based Microfluidic Sensors. Anal Chem. 2011; 83 (4):1300–1306. [PubMed: 21247195]
9. Li X, et al. Fabrication of paper-based microfluidic sensors by printing. Colloids and Surfaces B-Biointerfaces. 2010; 76(2):564–570.
10. Li X, et al. Quantitative biomarker assay with microfluidic paper-based analytical devices. Anal Bioanal Chem. 2010; 396(1):495–501. [PubMed: 19838826]
11. Dungchai W, et al. Use of multiple colorimetric indicators for paper-based microfluidic devices. Anal Chim Acta. 2010; 674(2):227–233. [PubMed: 20678634]
12. Wang W, et al. Tree-shaped paper strip for semiquantitative colorimetric detection of protein with self-calibration. J Chromatogr A. 2010; 1217(24):3896–3899. [PubMed: 20444459]
13. Martinez AW, et al. Programmable diagnostic devices made from paper and tape. Lab Chip. 2010; 10(19):2499–2504. [PubMed: 20672179]

14. Martinez AW, et al. Simple telemedicine for developing regions: Camera phones and paper-based microfluidic devices for real-time, off-site diagnosis. Anal Chem. 2008; 80(10):3699–3707. [PubMed: 18407617]
15. Martinez AW, et al. Three-dimensional microfluidic devices fabricated in layered paper and tape. Proc Natl Acad Sci U S A. 2008; 105(50):19606–19611. [PubMed: 19064929]
16. Abe K, et al. Inkjet-printed paperfluidic immunochemical sensing device. Anal Bioanal Chem. 2010; 398(2):885–893. [PubMed: 20652543]
17. Noh H, Phillips ST. Fluidic Timers for Time-Dependent, Point-of-Care Assays on Paper. Anal Chem. 2010; 82(19):8071–8078. [PubMed: 20809563]
18. Noh N, Phillips ST. Metering the Capillary-Driven Flow of Fluids in Paper-Based Microfluidic Devices. Anal Chem. 2010; 82 (10):4181–4187. [PubMed: 20411969]
19. Ballerini DR, et al. Flow control concepts for thread-based microfluidic devices. Biomicrofluidics. 2011; 5(1)
20. Reches M, et al. Thread as a Matrix for Biomedical Assays. ACS Appl Mater Interfaces. 2010; 2(6):1722–1728. [PubMed: 20496913]
21. Li X, et al. Thread as a Versatile Material for Low-Cost Microfluidic Diagnostics. ACS Appl Mater Interfaces. 2010; 2(1):1–6. [PubMed: 20356211]
22. Fu E, et al. Chemical signal amplification in two-dimensional paper networks. Sens Actuator B-Chem. 2010; 149(1):325–328.
23. Fu E, et al. Controlled reagent transport in disposable 2D paper networks. Lab Chip. 2010; 10(7): 918–920. [PubMed: 20300678]
24. Fu EL, et al. Transport in two-dimensional paper networks. Microfluid Nanofluid. 2011; 10(1):29–35. [PubMed: 22140373]
25. Osborn JL, et al. Microfluidics without pumps: reinventing the T-sensor and H-filter in paper networks. Lab Chip. 2010; 10(20):2659–2665. [PubMed: 20680208]
26. Kauffman P, et al. Visualization and measurement of flow in two-dimensional paper networks. Lab Chip. 2010; 10(19):2614–2617. [PubMed: 20676410]
27. Rasband, WS. ImageJ. US National Institutes of Health; Bethesda, Maryland, USA: 1997–2010.
28. Lucas R. Ueber das Zeitgesetz des Kapillaren Aufstiegs von Flussigkeiten. Kolloid Z. 1918; 23(15)
29. Washburn EW. The Dynamics of Capillary Flow. Phys Rev. 1921; 17(3):273.
30. Barry DA, et al. A Class of Exact-Solutions for Richards Equation. J Hydrol. 1993; 142(1–4):29–46.
31. Barry DA, et al. Comment on “An analytic solution of capillary rise restrained by gravity” by N. Fries and M. Dreyer. J Colloid Interface Sci. 2009; 338(1):293–295. [PubMed: 19589532]
32. Fries N, Dreyer M. An analytic solution of capillary rise restrained by gravity. J Colloid Interface Sci. 2008; 320(1):259–263. [PubMed: 18255086]
33. Perry, RH.; Green, DW. Perry’s Chemical Engineers’ Handbook. 7. McGraw-Hill; 1997.
34. Fenton EM, et al. Multiplex Lateral-Flow Test Strips Fabricated by Two-Dimensional Shaping. ACS Appl Mater Interfaces. 2009; 1(1):124–129. [PubMed: 20355763]
35. Lu Y, et al. Fabrication and Characterization of Paper-Based Microfluidics Prepared in Nitrocellulose Membrane By Wax Printing. Anal Chem. 2010; 82(1):329–335. [PubMed: 20000582]
36. Martinez AW, et al. Diagnostics for the Developing World: Microfluidic Paper-Based Analytical Devices. Anal Chem. 2010; 82(1):3–10. [PubMed: 20000334]

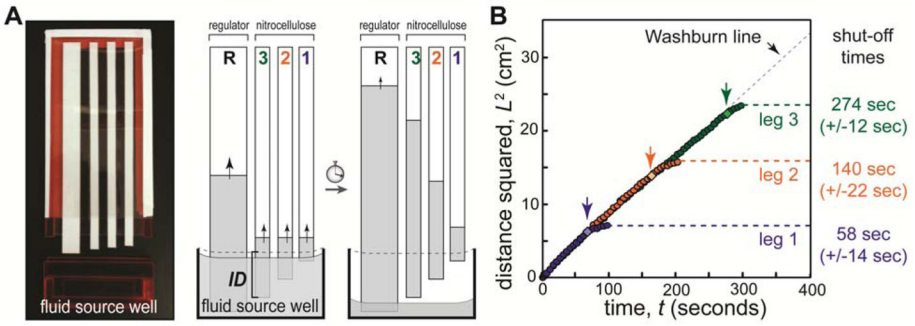

Figure 1.

Volume-limited well for programmed fluid shut off. A) Nitrocellulose legs (width 5 mm) were arranged on an adhesive plastic backing (cartridge) such that each leg protruded a different length. An optional high capacity cellulose regulating wick (width 1 cm) was added to increase the rate of fluid depletion from the well and to humidify the device. The source well (1 cm tall, 5 cm wide, 2.5 mm thick) was filled with buffer (PBST), and the cartridge was inserted to initiate flow. The cartridge interior thickness (air gap) was 1.5 mm. The leg immersion depth (*ID*) is indicated for leg 3; immersion depths were 3.5 mm, 4.5 mm, 5.5 mm for legs 1, 2, and 3, respectively. As fluid was wicked, each leg broke contact with the fluid in a timed sequence to provide programmed shut off. B) Plot of the fluid front position in each leg as a function of time. The fluid front in each leg followed Lucas-Washburn ($L^2 = Wt$) until it broke contact with the fluid in the well (indicated by light diamonds and arrows). The fluid front migrated somewhat after disconnection due to relaxation of fluid into the dry membrane. Relative errors in shut off times were 20%, 15%, and 5% for legs 1, 2 and 3, respectively.

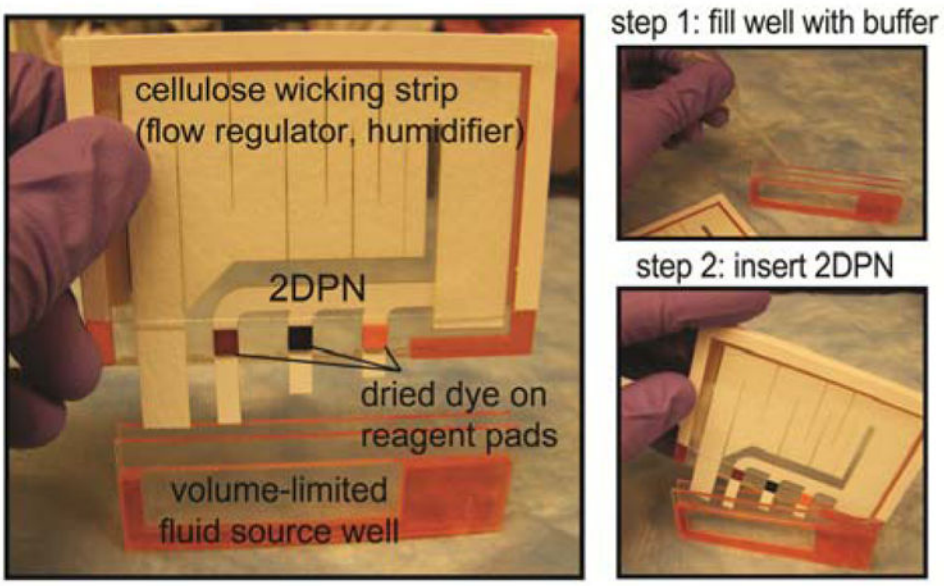

Figure 2.

A complete 2DPN for autonomous sequential fluid delivery. A) The 2DPN includes mock reagents (dyes) dried on pads and a regulating wick in a plastic housing. The cellulose wick regulated the fluid depletion rate, served as the downstream wicking pad, and humidified the device. Nitrocellulose legs: 0.5 cm wide, horizontal spacing 1 cm; leg immersion depths 4 mm (yellow), 7 mm (blue), and 13 mm (red). Regulating wick: cellulose, 1 cm wide at base. Reagent pads: 0.5cm x 0.5 cm cellulose with dried food colouring. Well dimensions: 6 cm wide x 1.5 cm tall x 2.5 mm thick; cartridge interior thickness (air gap): 1 mm. B) The device is operated by filling the self-metering well to capacity and inserting the 2DPN cartridge to initiate the sequence. The cartridge was designed to be fully inserted against a mechanical stop in the well, such that careful positioning by the user was not required.

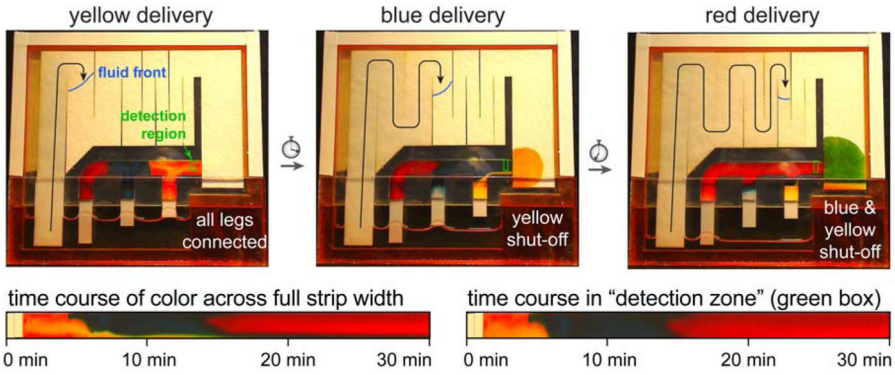

Figure 3.

Autonomous sequential fluid delivery in a 2DPN. Each leg wicked fluid from a single buffer source, and dried dyes representing reagents create different fluids from each leg (colours). Each coloured fluid arrived at a different time at the "detection zone" (green box) and was shut off in a timed sequence after delivery. Some "bleeding" from the cellulose reagent pads can be seen as a narrow band that occupies about 20% of the strip width. Time courses show colour across the full strip width or the detection zone as a function of time after device activation. Device dimensions are given in Figure 2. For perspective, the 2DPN shown here is ~2.5-fold larger in area than a conventional LFT (*e.g.*, LFT: 5mm x 40mm = 200mm^2; 2DPN paper area: 500mm^2), but smaller devices (2DPN and well) can be made if desired.